

## Scintillator detectors of AugerPrime

---

**Radomír Šmída<sup>\*a</sup> for the Pierre Auger Collaboration<sup>b</sup>**

<sup>a</sup>*Karlsruhe Institute of Technology, Karlsruhe, Germany*

<sup>b</sup>*Observatorio Pierre Auger, Av. San Martín Norte 304, 5613 Malargüe, Argentina*

*E-mail:* [auger\\_spokespersons@fnal.gov](mailto:auger_spokespersons@fnal.gov)

*Full author list:* [http://www.auger.org/archive/authors\\_icrc\\_2017.html](http://www.auger.org/archive/authors_icrc_2017.html)

As part of the upgrade of the Pierre Auger Observatory, called AugerPrime, scintillator detectors will be mounted on top of all water-Cherenkov detectors (WCDs) of the surface array. By combining the data from WCDs with those of scintillator surface detectors (SSDs), we can derive information needed to reconstruct the energy and composition of cosmic rays at energies higher than those reached by the Auger fluorescence telescopes. In this contribution, the mechanical structure of the SSDs and their optical properties are discussed. We also present novel techniques used in the construction of the prototype detectors deployed in the Engineering Array. The efficiency and light output of these detectors were measured using cosmic-ray muon tomography, providing an absolute calibration of the detectors at the same time. We have achieved  $\pm 10\%$  uniformity in the signal for particles impinging on any given detector at various impact points.

*35th International Cosmic Ray Conference — ICRC2017*

*10–20 July, 2017*

*Bexco, Busan, Korea*

---

<sup>\*</sup>Speaker.

## 1. Introduction

Information on the composition of cosmic rays, particularly at the highest energies, is of primary interest. Further studies of the origin and properties of the most energetic subatomic particles in the universe are substantially limited by the lack of composition information. Furthermore, the measurement of the fraction of protons is important for estimating the physics potential of existing and future cosmic-ray, neutrino, and gamma-ray detectors [1]. The composition has been studied up to the flux suppression region, i.e.  $\sim 4 \times 10^{19}$  eV, with the fluorescence detector (FD) [2] of the Pierre Auger Observatory [3]. To provide statistically significant composition information about primary particles in the flux suppression region, the Observatory is being upgraded with scintillator surface detectors (SSDs) and new electronics in water-Cherenkov detectors (WCDs) [1].

The SSD will provide a complementary measurement of extensive air shower particles to the data collected with the existing surface detector (SD). The sampling of secondary particles with two detectors having different responses to muons and electromagnetic particles is required to achieve accuracy on the composition comparable to the FD data. The design chosen for the SSD consists of a flat plastic scintillator positioned on top of every WCD. This design was selected because such a detector is reliable, low maintenance and cost effective. The area of the scintillator inside the SSD is  $3.8 \text{ m}^2$  in order for the statistical uncertainty to be comparable to that of the WCD.

The technical requirements on the SSD are manifold. The detector must be lightweight to avoid excessive stress on the plastic tanks installed in the Argentine Pampa for more than a decade. The total weight of one complete SSD is about 120 kg, which satisfies this requirement. The detector must be durable to withstand the harsh environment for at least seven years and of negligible maintenance. No complex production steps are desired and the same holds for the transportation and deployment.

Aluminum alloys have been selected as the most optimal material for the enclosure box, sun-roof and support frame of the SSD, because they satisfy the criteria described above and they have good corrosion resistance and strength. In addition, a custom profile can be easily extruded from aluminum alloy.

A drawing and a picture of the SSD on top of a WCD are shown in Fig. 1. The position of the SSD allows easy access to the dome housing the SD electronics and also to the SD photomultiplier tubes (PMTs).

## 2. Enclosure box

As can be seen in Fig. 2 the enclosure box is composed of a frame profile, an aluminum composite panel and a top sheet. These components, made primarily from aluminum, make a water-tight housing for plastic scintillator bars, fibers and a PMT with electronics.

The frame profile is custom extruded and its double wall structure provides additional strength for the module and the place for installing closed-end blind rivets. Each wall is 83 mm high and 2 mm thick and the space between two two walls is 26 mm. The thickness of the top part of the rectangular profile is 2 mm and 3 mm at the bottom. The bottom part of the extruded profile frame protrudes inward 30 mm and supports the aluminum composite panel. Four beams, two 3800 mm

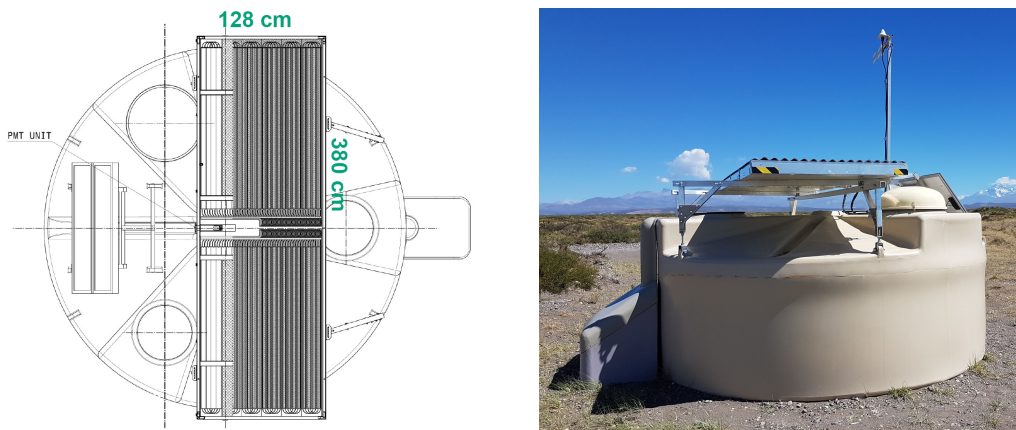


**Figure 1:** Drawing of an open SSD on top of a WCD (*left*) and a photo of one installed SSD (*right*).

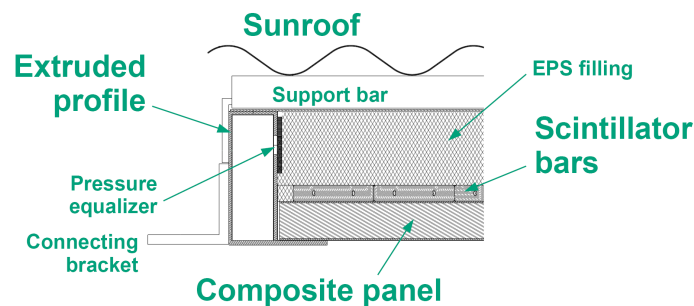


**Figure 2:** Side-view cut in the drawing of the SSD. Main parts are marked.

and the other two 1280 mm long, are connected in two ways depending on the assembly site: corner inserts and nails are used in the first case and corners are welded in the second case.

The composite panel has two 1 mm thick aluminum sheets glued to a 22 mm thick block of extruded polystyrene (XPS). The panel is glued to the frame with Ottocoll S610, which acts also as a sealant. The panel not only increases the structural integrity, but its flat area is convenient for placing components inside the box during assembling. Four aluminum U-beams fix the scintillator bars from above and lightweight blocks of expanded polystyrene (EPS) are used to fill the space.

The air volume inside the detector is reduced to less than 10 liters this way and a top sheet is supported from below. The exchange of air between the outside and the inside of the detector is achieved via a couple of holes at the bottom of the profile frame and one hole in the inner wall of the profile. The latter hole has a diameter of 12 mm and is covered with a round piece of sintered metal. This system acts as a pressure equalizer.

The top of the box is closed with a 1 mm thick aluminum sheet. This top sheet is glued to the frame profile with the same glue as the panel and in addition, the connection is reinforced with closed-end blind rivets. Even though the first shipment of SSDs had experienced acceleration up to 15 g during transportation, these acceleration shocks had caused no damage.

### 3. Sunroof

The main purpose of the sunroof is to deflect sunlight and keep excursions of the temperature inside the detector below 50°C as can be seen in the top graph in Fig. 7. The sunroof is made from corrugated sheets and the air flow under it provides passive cooling, keeping the SSD at around the temperature of the ambient air.

The roof is riveted to six support bars fixed on top of the enclosure box. These six rectangular beams are connected to the frame with angles riveted to the outer wall and they are also glued to the top sheet. The beams support the sunroof and in addition they hold and reduce any vibration of the almost 5 m<sup>2</sup> large top sheet.

### 4. Support frame

The support frame holds the SSD in the horizontal position on top of the SD. It must be adjustable enough to compensate for deformations of the plastic tanks standing on the sandy ground for more than a decade. It is made from aluminum beams and can be easily assembled. Two shorter beams are fixed to the main beam and this structure is supported by four legs connected to lifting lugs molded into the plastic tank.

The enclosure box is placed on top of the already mounted support frame with a jib crane installed on a pickup truck. The box has two brackets riveted to its two long sides and it is going to be fixed with screws to the support frame in these four positions. The installation procedure takes only about ten minutes. An SSD installed on WCD is shown in the right picture in Fig. 1

### 5. Scintillators and fibers

The active area of the detector is made from extruded scintillator bars produced at the Fermi National Accelerator Laboratory, USA [4]. Each bar is 1600 mm long, 50 mm wide and 10 mm thick. There are 48 pieces in an SSD distributed equally between two wings. Two bean-shape holes are inside each bar at the distance of 25 mm from each other. A TiO<sub>2</sub> layer with a typical thickness of 0.25 mm is co-extruded on the bar. This outer layer protects bars from damage during handling, prevents cross talk between bars and due to its high diffuse reflectivity increases the collected signal. The total area of the scintillators is 3.8 m<sup>2</sup>. The emission lines of the scintillator material lie between 330 and 480 nm, but all light emitted below 400 nm is attenuated within a 10 mm path length of the scintillator.

Plastic wavelength shifting (WLS) fibers are used to collect sufficient light signal. The total length of each fiber is about 5.8 m. The fiber Kuraray Y11(300)M, S type of 1 mm diameter is used in the SSD [5]. The absorption spectrum of this WLS fiber matches the emission spectrum of the scintillator material. The light emitted by the fiber has wavelengths above 450 nm.

The fiber is pushed through one of the holes in a scintillator bar and guided in a router to a hole in another scintillator bar. The second hole is at a distance of 100 mm from the first hole to comply with the recommended minimum bending diameter for low light loss due to bending and long term reliability. This U-turn is shown in Fig. 3. In the center of the SSD all the fibers are guided in routers and collected in a bundle in a cookie, a housing made from PMMA, where

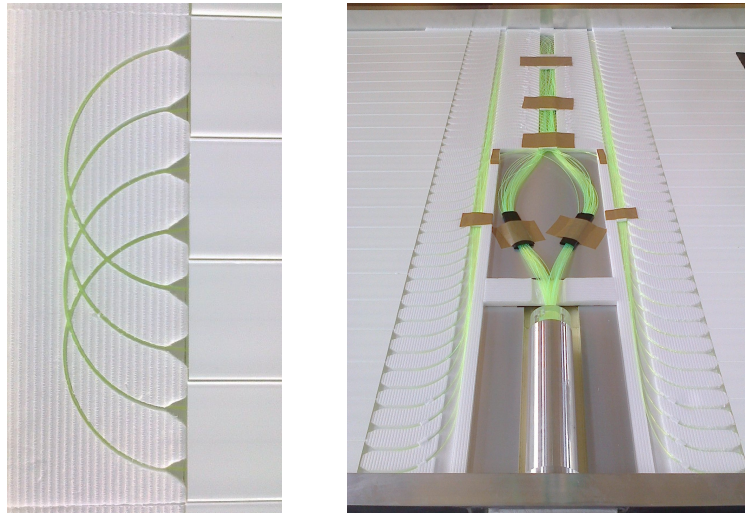


**Figure 3:** Routers for guiding and protecting fibers on the side (*left*) and in the center (*right*).

both ends of each fiber end. The length of the fiber between the scintillator bar and the cookie is about 1.1 m, see the right picture in Fig. 3. Therefore, only photons with the wavelength above  $\sim 500$  nm survive the whole path, because of their sufficiently long attenuation length. Owing to the guiding in routers, no significant light loss due to bending happens in any part of the fiber over its whole length. The routers also keep fibers in their position and reduce the risk of damage during subsequent procedures.

Almost one half of light is lost, if a fiber's end surface is not finished after cutting. A novel method has been developed for finishing the 96 ends of plastic WLS fibers already installed in the SSD. This procedure is based on melting each end of a fiber on a borosilicate glass plate warmed to  $150 \pm 30^\circ\text{C}$ . The end of the fiber, held by hand, is touched for about one second to the glass plate. Its surface slightly melts and flattens. The advantages of this procedure are as follows: easy and simple, the required time for melting can be checked visually<sup>1</sup> and any defect (e.g. a bubble due to a too long contact with the plate) can be repaired by cutting a small piece of the fiber and repeating the procedure. In Fig. 4 the end of a fiber before and after melting is shown. We have verified that the fiber finished with the melting method provides within 10% the same amount of light as a carefully polished fiber. This new procedure is less labor intensive than polishing all 96 ends of the fibers glued in the cookie at once.

The ends of all fibers are bundled in the cookie, which has a body and front window made of PMMA. The hole for fibers in the center of the PMMA body has a diameter of 13 mm and two smaller holes along it for filling optical cement and allowing air to escape. The fiber ends are aligned 1 – 2 mm in front of the window which is pushed into the main body. This front window has a diameter of 22 mm and a thickness of 6 mm, and it will protect the ends of the fibers and act as a diffuser. At the end, the optical cement (we use Eljen EJ-500) is poured inside – slowly, to avoid air bubbles forming in front of the fibers.

<sup>1</sup>A clear decrease in the amount of side-scattered light can be observed during the melting of a fiber. Side-scattering is caused by surface roughness after cutting a fiber.

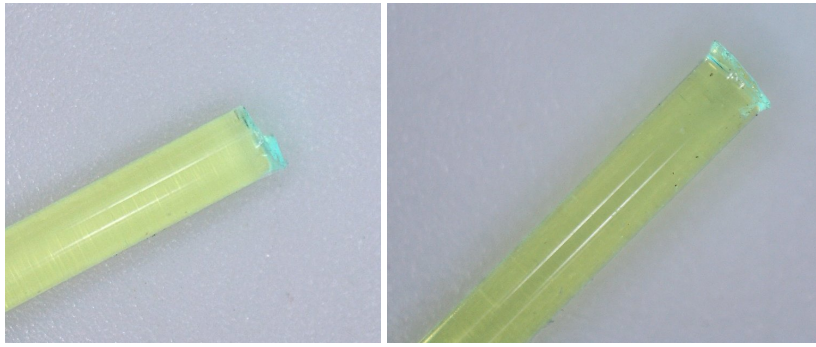


**Figure 4:** A fiber's end after cutting (*left*) and after finishing with the melting procedure (*right*).

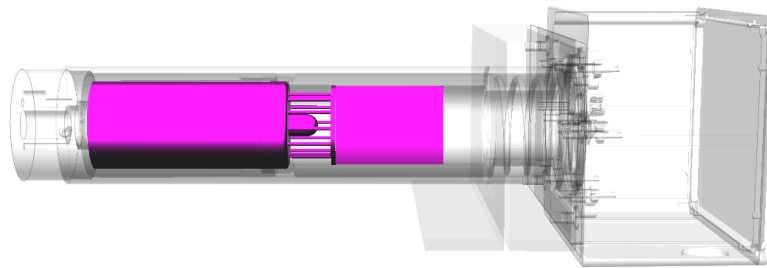


**Figure 5:** The housing of a PMT. The PMMA cookie in the front of the aluminum tube and the PMT with the integrated HVPS are highlighted, visible are also the spring and flange with connectors and the protection box on the right side. Cables are not included here.

## 6. Photomultiplier tube

A photomultiplier tube (PMT) measures the signal delivered from the scintillators with fibers. The main candidate for the PMT is the model Hamamatsu R9420. It is a 1.5" PMT with a standard bialkali photocathode and a quantum efficiency of about 18% at the wavelength of 500 nm. The dynode chain has eight stages. The PMT provides the required linearity range at the operating PMT gain  $\sim 7 \times 10^5$  [1, 6, 7]. The high voltage power supply (HVPS) is based on a custom-made design manufactured by the ISEG company. As a backup, the PMT ET Enterprises 9902B is considered. The PMT signal will be read out with the upgraded SD electronics presented in [1, 8].

An important design criterion on a PMT module was the ability to remove the PMT from the SSD. This has been accomplished by housing the PMT, the HVPS and accompanying electronics in a PVC tube. The PVC tube can be easily installed and removed from the aluminum tube, which is permanently fixed in the profile frame, see Fig. 5 and the bottom of the right picture in Fig. 3. The PMT is pressed with a spring to the cookie, where a silicone pad makes an optical connection which also distributes any pressure over the entrance glass window of the PMT. The inner volume of the aluminum tube is closed with a flange equipped with an SMA and multipole connector for an analog signal and a slow control cable, respectively. The weather protection of the connectors is guaranteed by an aluminum cover box.

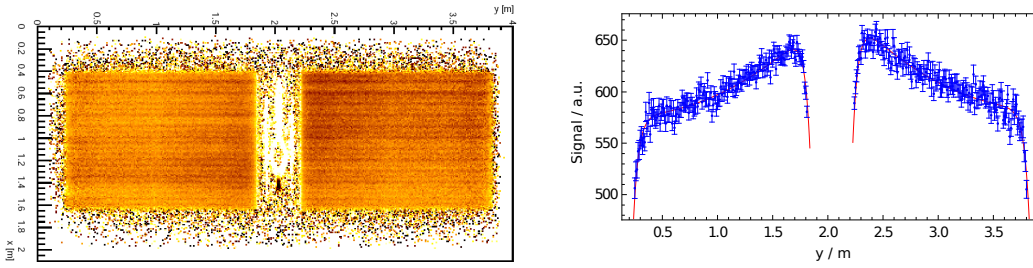


**Figure 6:** *Left:* Logarithm of the signal charge measured in the muon telescope. Individual scintillator bars and bundles of fibers in the center can be recognized. Compare with the right picture in Fig. 3. *Right:* The signal measured for MIPs along the long axis of scintillator bars for two halves of the SSD. The PMT is located at  $y = 2$  m.

## 7. Testing

Tomography with cosmic-background muons has been used to test all assembled SSDs, see Fig. 6. The spatially sensitive muon telescope used for this purpose came from the KASCADE experiment [9]. It consists of three  $2\text{ m} \times 4\text{ m}$  plates vertically separated by 1 m. A spatial resolution of  $\sim 10$  mm can be achieved for a particle measured in all three layers. Some detectors were studied in multi-day runs and these data allow a detailed study of the signal from individual fibers.

The charge of a single photoelectron and a minimum ionizing particle (MIP) have been measured in the same configuration for all SSDs. From these two charges, the number of photoelectrons (p.e.) has been calculated for each MIP and converted to a vertical-equivalent MIP (VMIP). The fit of measured signals with the Gaussian function gives  $30 \pm 2$  p.e./VMIP, while the mean signal is 37 p.e./VMIP.

Due to the U-turns of the fibers and their sufficient length outside of the scintillator bars, the uniformity of the measured signal is  $\pm 5\%$  along bars and  $\pm 10\%$  between bars for MIPs depositing signal at any position of the detector, see the right picture in Fig. 6. We can conclude that the response of the detector will be uniform for all measured particles of an extensive air shower.

The length and shape of pulses have also been studied. The signal is wider and narrower at the close and far end of the detector, respectively. The attenuation length of the light in a fiber is  $\lambda = 312 \pm 3$  cm and the effective index of refraction is  $n \simeq 1.76$ .

Results of the measurements have been fully implemented in our Offline framework [10].

## 8. Performance and Conclusions

Twelve scintillator detectors were deployed in the Engineering Array in the middle of September 2016 and have been taking air shower data since October of the same year. Due to the deployment in an easily accessible part of the Observatory, six detectors were installed during one day. No issue with either mechanics or performance has been noticed after almost half a year and all SSDs fulfill our requirements. The SSDs have provided first results, which have been presented in [11].

Each SSD is equipped inside with two temperature sensors and a humidity sensor. As can be seen in the top graph in Fig. 7, the temperature inside the enclosure box closely follows the air

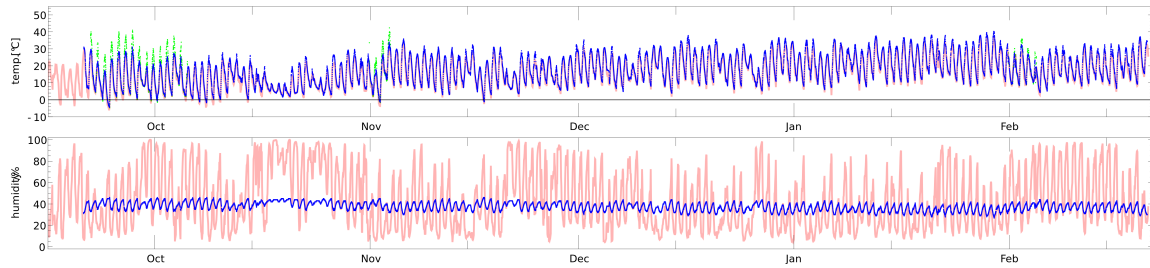


**Figure 7:** *Top:* Temperatures inside and outside an SSD (measured in the shade) are shown in blue and red color, respectively. Green points correspond to temperatures in direct sunlight. *Bottom:* Humidities inside and outside an SSD are shown in blue and red color, respectively.

temperature measured in the shade and only rarely exceeded  $40^{\circ}\text{C}$ . The evolution of the humidity can be seen in the same figure. The humidity has been slowly decreasing from the original value of  $\sim 40\%$ , see the bottom graph in Fig. 7.

The SSDs for the AugerPrime will be produced in different facilities around the globe. On average, about one SSD can be produced at each facility per day, which is sufficient to produce all detectors for AugerPrime within the next two years.

## References

- [1] Pierre Auger Collab., Preliminary Design Report, arXiv:1604.03637.
- [2] Pierre Auger Collab., Phys. Rev. D 90 (2014) 122005.
- [3] Pierre Auger Collab., Nucl. Instrum. Meth. A 798 (2015) 172.
- [4] A. Pla-Dalmau *et al.*, FERMILAB-Conf-03-318-E.
- [5] <http://kuraraypsf.jp/psf/ws.html>
- [6] D. Martello, for the Pierre Auger Collaboration, PoS (ICRC2017) 383.
- [7] A. Castellina, for the Pierre Auger Collaboration, PoS (ICRC2017) 397.
- [8] T. Suomijarvi, for the Pierre Auger Collaboration, PoS (ICRC2017) 450.
- [9] P. Doll *et al.*, Nucl. Instrum. Meth. A 488 (2002) 517.
- [10] D. Schmidt, for the Pierre Auger Collaboration, PoS (ICRC2017) 353.
- [11] Z. Zong, for the Pierre Auger Collaboration, PoS (ICRC2017) 449.